AIMS Geosciences, 6(3): 298–315.
DOI: 10.3934/geosci.2020018
Received: 30 June 2020
Accepted: 12 August 2020
Published: 20 August 2020

http://www.aimspress.com/journal/geosciences

Research article

Sedimentation in the Bay of Samaná, Dominican Republic (1900–2016)

Ramón Delanoy[1,*], Misael Díaz-Asencio[2] and Rafael Méndez-Tejeda[3,*]

[1] Institute of Physics, Faculty of Sciences, University of Santo Domingo. Santo Domingo. Dominican Republic
[2] Division of Oceanology, Center for Scientific Research and Higher Education at Ensenada (CICESE), Ensenada, Baja California, Mexico
[3] Research Laboratory in Atmospherical Science, University of Puerto Rico at Carolina, Carolina Puerto Rico

* **Correspondence**: E-mail: rdelanoy67@uasd.edu.do; rafael.mendez@upr.edu.

Abstract: The purpose of this article is to provide an analysis of the geochemistry of sediments deposited in the Bay of Samaná (Dominican Republic) after 1900, emphasizing in the recent changes (last 20 years). This bay was formed by tectonism and sedimentation that joined the Samaná peninsula with the northern mountain range.

From 2003 to 2016, Dominican Republic was impacted by several cyclonic systems (storms and hurricanes), which caused an increase in the runoff of all rivers and streams that flow into the coastal area by depositing large amount of sediments in the basins of the rivers and tributaries. The Sedimentary Accumulation Rate (SAR) found in the cores indicates an increase in runoff which resulted in a decrease in the area and depth of the bay where sediment was deposited by rivers and streams.

When analyzing data from the period 2003 to 2019, it was observed that the Yuna River has made an intrusion of sediment displacing 2.38 km^2 to the bay, its average SAR was 1.78 cm per year (cm y^{-1}). The main cause of this increase in sediment deposition was mining, followed by deforestation, agriculture, and urban planning over the years, all activities that have the common denominator of being anthropic.

Keywords: sediment; Bay of Samaná; Dominican Republic and runoff

1. Introduction

Hispaniola is an island in the Greater Antilles on which two countries coexist, Haiti (West) and the Dominican Republic (East). This island is of tectonic origin arising from the volcanism of the region during the Cretaceous period of the Mesozoic era and by sedimentation in the recent Quaternary [1–3]. The Bay of Samaná is located in the Dominican Republic (Figure 1). A portion of the sediment in the bay has been caused by landslides in the steep areas of the Samaná peninsula and is washed away by rivers and streams in the northern part of the bay [4]. These trawls are important factors in the degradation of water quality and the bay environmental and ecological conditions [5,6]; however, the greatest contributions of dragged soils, which change the coastal area, are generated from the basins of the Yuna-Camú, Yabón, Caño Hondo, and Yeguada Rivers that flow into the southern slope of the Bay of Samaná [7,8] and the Samaná River that flows in from the northwest.

Figure 1. Map of the Caribbean region. The box is the location of the Bay of Samaná in the Dominican Republic, as well as the location from where the cores were retrieved. Source: Google maps.

Environmental reconstructions in sediment have been carried out with success by [9] and more recently by [10] using radiometric dating techniques to evaluate sediment deposition time. The dates obtained from the dating with ^{210}Pb (natural radionuclide of the ^{238}U decay chain) can be used to reconstruct the past (up to 150 years) using the sediments as environmental archives [11–13]. This period is sufficient since industrial development activities and population growth in the region have occurred in the last eight decades (National Statistics Office, Dominican Republic).

The study of sediments can provide current and past information because the sediment transported from various rivers supply historical records of the geological and hydrological condition of the basin over time [14], the sedimentary accumulation rate (SAR) [15] and, the composition and enrichment of pollutants [16]. These parameters directly related to the displacement of soil masses either by landslides or by erosion during rain, which intensify during storms or hurricanes are considered extreme weather events (EWE). In recent years, there has been an increase in these extreme events observed [17]. The 2004 to 2012 was predominantly influenced by La Niña and the Bay of Samaná was significantly impacted at this time [18].

EWEs are frequent in the Dominican Republic because of the island is located in relation to the routes of tropical waves, hurricanes, and storms that form in the south-central tropical zone of the Atlantic and are dragged by trade winds to the northwest. The contributions of sediment by the rivers from storms during the 2004–2012 period were very noticeable [19]. The same happened with the passage of Hurricane Irma and María that affected Puerto Rico in September 2017. The Bay of Samaná is economically important for the Dominican Republic. The bay is known for many sightings of humpback whales, which in late winter and early spring remain in the waters of the bay to reproduce. Tourism, fishing, and agriculture are the most important economic sources of livelihood in the towns of Sánchez, Samaná, Sabana de la Mar and Miches, which is why it is important to study sedimentation as an element of ecosystem degradation (coastal zone and biodiversity) [20].

The purpose of this article is to analyze the geochemistry and sedimentation rate in Samaná Bay, after 1900, emphasizing in recent changes in the last two decades and to infer their relationship with the EWEs. We identified the more affected zones by runoff and interpreted the main cause associated with human activities

2. Materials and method

2.1. Study area

The geographic location of the bay is delimited to the North by the peninsula of the same name, to the South by the North slope of the eastern mountain range and Los Haitises National Park, to the East by the Atlantic Ocean, and to the West by the old Great Estero, now called El Bajo Yuna [1]. The Yuna River and its tributaries, the Camú and Jayas Rivers, cross the central Cibao region collecting the waters from the provinces of Monseñor Noüel, Duarte, Sánchez Ramírez, and La Vega (Figure 2), and their runoffs bring large deposits of sediment to the Bay of Samaná [21].

In these provinces there are important human settlements dedicated to agriculture, livestock, and mining that contribute to soil erosion and water pollution [22]. To the South of the bay, the Sabana la Mar and Miches towns are the main contributors to the sediment trawls of the Yabón and La Yeguada Rivers, respectively [23].

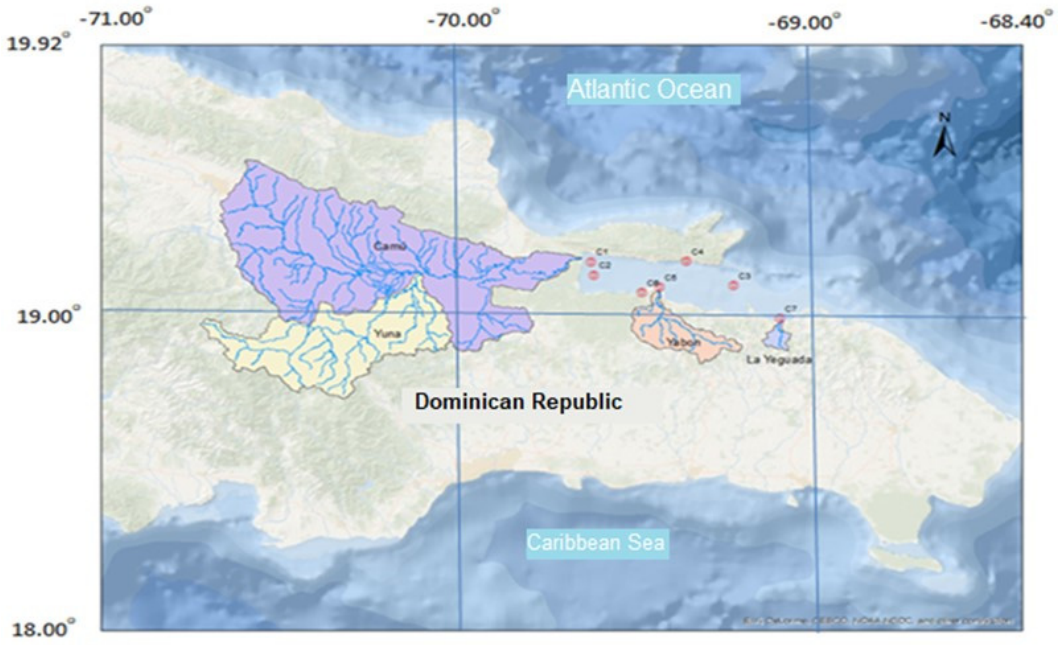

Figure 2. Map of the Dominican Republic showing Yuna, Camú, Yabón, and Yeguada Rivers Basin and core locations. Map modified from Andrés Moreta (2002).

2.1.1. Regional geological conditions

The Yuna river that crosses the Nickel mining area in Bonao and the Gold one in Maimon as well as the main rice and banana crops in the country; where the Cibao valley meets the eastern mountain range in the vicinity of Cotuí. There are also massive limestones with rudists and dark limestones with silex nodules from the Albian age, as well as karstified limestones from Los Haitises and clayey alluvium from the Quaternary trawls of the Camú and Yuna rivers in the Lower Yuna region and the middle basin, affect sediment texture as well as grain size [24]. In the Miches Zone there are deposits of volcanic and volcano-sedimentary materials, as well as sedimentary reef limestones during the Aptian-Albian. Sandstones and tuffs deposited in a turbiditic environment during the Upper Cretaceous; the group is affected by small serpentinite and diabase intrusions forming conglomerates [23].

The Samaná Peninsula formed by Miocene-Pliocene siliciclastic rocks that have been transformed. There are also marine Quaternary terraces, made up of stratified limestones where algae, mollusks and corals are found [25]. The rocks of the Sánchez area composed of lignite and mud constituted of a high content of organic matter, as they are a deposit of remains of the fauna and flora of the reef area of the bay as they are sedimented in this area in the Miocene. It was tertiary when the Peninsula was separated from the Cordillera Septentrional forming the great estuary. The peninsula presents several inverse North-South faults that are concurrent to the North fault, which is a sliding one, predominantly in the East-West direction. Further South of the bay is the continuation of the Cibao fault and also the Yabón fault, in the southeast-northeast direction. The peninsula is part of the ridged block in the subduction zone that is located northeast of Hispaniola [25].

The main tributaries to the Samaná Bay from the northern side are the Majagual River and a series of small streams between the towns of Majagual and Sánchez, with North-South direction and subject to minimal travel. Water from several of these streams flows into the Yuna near the mouth. Other tributaries are located between the towns of Sánchez and Punta Balandra (Punta Gorda, Higüero, Salado, Hondo, Juana Vicenta, Las Flechas, Los Cacaos, and Los Limones), and the Santa Capuza, Los Cocos, Bushi and Balandra Rivers, heading North-South and little travel. These rivers and streams drag the sediments of the peninsula and the wastewater of the towns located along the coastal zone (Table 1).

2.1.2. River Yuna-Camu

The river basin of the Yuna River is formed by Cibao south-central, northeast and part of the Cibao north-central region. The area of the basin is 5253 km^2 and is formed by a broadleaf forest that occupies about 44% (2311 km^2) of the Yuna basin. The remaining 56% is dedicated to four types of agricultural use: intensive crops (848.6 km^2), pastures (634.2 km^2), rice (607.3 km^2), and cocoa (530.7 km^2). The high areas of the Central mountain range and the Yamasá mountain range are covered by 190.3 km^2 of coniferous forest (3.6%) [26,27]. Ferro-nickel and gold mines operate at the Yuna basin.

2.1.3. River La Yeguada (Miches)

The Yeguada River, in the Yuma region, is located in the El Seibo province and flows into the municipality of Miches. The area of the basin is 53.7 km^2. Cocoa plantations are the main land use coverage in the La Yeguada River basin covering an area of 26.5 km^2, which is 49% of the land. The broad and humid broadleaf forests cover 36% (19.3 km^2) of the basin. Grass is another land use covering about 7 km^2 (13%) [26].

2.1.4. River Yabón (Sabana de la Mar)

The Yabón River, in the Higüamo and Yuma regions, is located in the provinces of Hato Mayor and El Seibo. The area of the basin is 370.6 km^2. The majority of the land, about 107.2 km^2 (29%), is dedicated to the cultivation of cocoa, followed by wet broadleaf forest that comprises 85.2 km^2 (23%) of the territory. Grass occupies third place with 71.8 km^2, making up 19% of the land. Lesser uses for the land are dry scrub, coconut, and intensive crops [26].

2.2. Sampling

Using the UWITEC gravity corer, seven sediment cores were collected in the study area near the mouths of the main rivers (Yuna, Yabón, La Yeguada, Caño Hondo, and Samaná) and one inside the bay (Table 1, Figure 2). The cores were extracted manually and then cut into sections of 1 and 2 cm according to the length of the core [1].

Table 1. Location, length, and depth of cores taken from the coastal areas, the Bay of Samaná.

Station code	Latitude (N)	Length (W)	Core length (cm)	Depth (m)	Site
C1	19.1926	69.5977	100	28	Yuna-Barracote River mouth
C2	19.146	69.5913	82	25	Yuna River mouth
C3	19.1095	69.1805	46	12	North Miches
C4	19.1933	69.3198	58	5	Puerto Samaná
C5	19.1041	69.3977	92	15	Yabón River
C6	19.0851	69.4492	52	6	Caño Hondo River
C7	18.9958	69.0452	20	6	Yeguada River mouth

2.3. Analytical methods

2.3.1. Moisture content and loss of ignition

The sediments were weighed wet and dry at a temperature below 50 °C in an oven to determine the moisture content, up to constant weight after several weightings. A portion of 3 grams of dry weight was incinerated at a temperature of 450 °C in a flask to determine the content of organic matter [28,29].

2.3.2. Chemical composition

A 3-gram portion of the dried, crushed, and sieved sample was pressed into a tablet. The tablet was placed on the Skyray-Instrument EDX-RF 36000B X-ray fluorescence spectrometer to determine the concentration of chemical elements from sodium to uranium. The elements that we were interested in analyzing were Cr, Cu, Pb, Hg, Zn, Ni, Mn, Fe and Ca. The spectrometer was previously calibrated using standard sediment samples certified according to ISO/IEC 17025 and ISO Guide 34 by Sigma-Aldrich (TraceCert; NIST, IAEA) and BAM-CRM (SRM1944, SRM2707, SRM1646a and IAEA356). The quality of the heavy metal determinations of the sediment equipment was verified using the BCR277 and SRM1944 certified materials [1].

2.3.3. ^{210}Pb excess analysis

Approximately 1.0 gram of dried, crushed, and screened sample was completely digested by the EPA-3050B method, using a mixture of nitric acid and concentrated hydrochloric acid. First, by adding the hydrochloric acid little by little until the effervescence was completely eliminated due to calcium carbonate and then by adding the nitric acid. Using a Thriathler liquid scintillation counter, the beta emissions of the digested material from ^{210}Bi were determined in secular equilibrium with ^{210}Pb after 15 days of preparing the samples [30,31]. In this way, the beta activity was determined [32], with the objective of determining the deposition date of each sediment section from the decay of ^{210}Pb in excess and its half-life [33,12].

2.4. Data analyses

Using satellite and aerial photos, comparisons of the coastline were made to recent years. Photos were taken during periods when there were incidents of meteorological events in the region and compared with changes in coastlines and sedimentation rate. Furthermore, we compare the trends between sediment composition and sedimentary accumulation rate (SAR), previously reported for us in these sediment cores [1].

3. Results and discussion

3.1. General compositions in sediment cores

Table 2 showed the values of major and trace element (0–10 cm) in the seven cores collected in the study area analyzed by XRF, values were recovered from a previous research [1].

The average concentrations in the seven sediment cores (0–10 cm) showed a significant variation of the sediment composition in the study area (Table 3). The cores C1 and C2, recovered at the current and old mouths of the Yuna River, showed high concentrations of Cr and Ni, with values higher than the PEL in all samples for both elements, and high levels of Zn. For Cr and Ni, we observed significant enrichment respect to the Upper Continental Crust (UCC) and values reported in other bays in the world (Table 4). In C1, we found also elevated levels of Hg and Pb. The trace elements in core C1 showed the highest concentrations of all trace elements, due to the origin of the sediments carried by the Yuna; mining areas, towns and agricultural crops.

The core C3, collected in the North of Miches, contained more than 40% of Ca on average (0–10 cm), indicating that sediments are of marine origin with clay texture and debris of corals. The Fe is 0.6%; it is the lowest value in all sediment cores. The trace elements showed content lower than the values reported in the UCC and other bays in the world (Table 4). In this area, no enrichment of trace elements was found. In the core C4, taken at the Port of Santa Bárbara de Samaná values of Cr and Ni were very higher, with elevated values of Pb (>PEL). In this site, trace elements concentrations were similar to C1 and C2, but with relatively low values of Zn and without Cu content.

In the cores C5 and C6, only Cr and Ni showed an enrichment respect to the Upper Continental Crust and values report in other bays (Table 4). The C7 collected at the mouth of the La Yeguada river in Miches, had 14.6% of Ca and 1.4% of Fe; we found an enrichment of Cr and Ni, with significantly higher levels of Hg.

Table 2. Major and trace elements in the sediment cores taken in the bay of Samaná.

Core	Depth (cm)	PPI	Ca %	Fe %	Mn %	Cr µg/g	Ni µg/g	Cu µg/g	Zn µg/g	Hg µg/g	Pb µg/g
C1	0	17.1	2.2	6.3	0.07	253.2	95.2	70.6	105.8	1.7	24.0
	2	19.3	2.5	6.6	0.07	329.8	118.0	37.0	92.6	1.6	21.5
	4	19.1	2.4	6.6	0.05	203.5	139.5	99.4	75.8	1.0	27.2
	6		2.6	7.2	0.08	260.0	131.6	74.8	114.0	*	41.5
	8		2.4	6.7	0.06	364.8	116.4	90.6	162.0	*	21.4
	10		2.4	6.6	0.05	155.1	99.4	54.1	131.0	*	34.7
C2	0	14.8	1.8	5.1	0.04	190.1	86.1	44.3	119.0	*	8.7
	2	13.2	1.5	5.2	0.04	85.3	117.2	13.9	148.1	*	4.5
	4	12.6	1.7	5.1	0.04	176.6	118.0	47.8	216.3	*	8.7
	6	12.7	2.0	5.1	0.05	191.4	116.1	9.8	203.8	*	8.0
	8	13.7	2.0	5.2	0.05	186.0	114.9	34.4	182.3	*	6.2
	10	13.6	2.2	5.3	0.05	164.5	85.4	49.8	119.4	*	3.7
C3	0	12.0	42.9	0.7	0.02	10.9	28.7	18.4	36.8	*	7.6
	2	10.8	41.8	0.6	0.01	5.5	36.9	8.8	37.5	*	6.3
	4	13.6	43.0	0.7	0.01	27.3	31.3	6.7	33.2	*	4.7
	6		41.7	0.7	0.01	46.1	20.3	9.2	35.1	*	2.8
	8	11.9	44.9	0.6	0.01	10.9	27.7	9.6	36.1	*	6.8
	10		44.8	0.7	0.01	50.0	15.6	8.3	37.0	*	4.4
C4	0	16.9	3.1	3.2	0.05	258.1	93.7	*	42.5	*	36.7
	2	16.6	3.4	3.1	0.05	171.4	149.4	*	54.6	1.4	21.2
	4	18.3	2.9	2.8	0.04	193.9	139.0	*	47.4	*	30.2
	6	16.8	3.5	3.0	0.04	200.6	164.1	*	40.8	*	35.2
	8	21.0	3.6	3.3	0.05	188.6	71.1	*	58.1	*	32.2
	10	15.9	3.4	3.3	0.05	194.6	131.4	*	52.3	*	44.1
C5	0		1.3	4.9	0.07	108.9	46.1	*	24.9	*	
	2	16.4	1.0	4.9	0.07	158.7	93.5	*	22.4	*	11.8
	4	14.6	1.1	5.2	0.07	116.4	32.3	*	28.1	*	11.5
	6	20.0	0.6	2.6	0.03	49.9	51.8	*	8.3	*	14.1
	8	15.4	2.1	4.5	0.06	57.9	123.6	*	27.9	*	15.2
	10	20.8	2.0	4.2	0.07	44.0	74.5	*	11.8	*	16.0
C6	0	14.4	1.2	4.5	0.06	193.0	75.1	*	18.7	*	6.7
	2	13.9	1.2	4.5	0.05	259.2	32.6	*	17.3	*	7.1
	4		1.3	4.6	0.05	205.7	73.7	*	15.2	*	10.5
	6	13.5	1.4	4.6	0.05	181.3	81.4	*	11.5	*	7.3
	8		1.3	4.7	0.04	281.2	79.2	*	24.8	*	11.7
	10	13.4	1.2	4.5	0.05	220.9	80.4	*	11.1	*	14.9
C7	0	11.2	17.4	1.1	0.04	64.1	113.4	*	*	1.4	0.0
	2	9.5	9.8	2.1	0.05	103.0	87.0	*	*	2.2	20.0
	4	7.9	10.1	2.0	0.05	108.5	112.4	*	*	*	22.6
	6	7.6	17.8	0.9	0.03	65.7	54.0	*	*	*	11.2
	8	8.5	17.0	1.0	0.03	68.4	99.9	*	*	*	3.1
	10	15.2	15.5	1.3	0.04	69.0	109.2	*	*	1.4	4.0

** Concentrations < LD*

Table 3. Range of major and trace elements in the sediment cores. Allowable exposure limits (PEL) and effect threshold level (TEL), SQuiRTs-NOAA [34].

			Level Range in each Core (µg/g)													
	PEL	TEL	C1		C2		C3		C4		C5		C6		C7	
Element	µg/g	µg/g	Min	Max	Min	Max	Min	Max	Min	Max	Min	Max	Min	Max	Min	Max
Cr	52	160	155	365	85	191	6	50	171	258	44	159	181	281	64	109
Ni	16	43	95	140	85	118	16	37	71	164	32	124	33	81	54	113
Cu	19	108	37	99	10	50	7	18	*	*	*	*	*	*	*	*
Zn	124	271	76	162	119	216	33	38	41	58	8	28	11	25	0	0
Hg	0.1	0.7	1.0	1.7	*	*	*	*	1.4	1.4	*	*	*	*	1.4	2.2
Pb	30	112	21	42	4	9	3	8	21	44	12	16	7	15	0.0	23
			Level Range in each Core (%)													
Ca			2.2	2.6	1.5	2.2	41.7	44.9	2.9	3.6	0.6	2.1	1.2	1.4	9.8	17.8
Fe			6.3	7.2	5.1	5.3	0.6	0.7	2.8	3.3	2.6	5.2	4.5	4.7	0.9	2.1
Mn			0.05	0.07	0.04	0.05	0.01	0.02	0.05	0.05	0.03	0.07	0.04	0.06	0.03	0.05

** Concentrations < LD.*

Table 4. Average concentrations of trace elements (mg kg^{-1}) in the sediment of the Bay of Samaná, in the Upper Continental Crust (UCC) [35], and in other bays around the world [36–40].

Site		Range of trace elements				
sediment cores		Cr	Ni	Zn	Pb	Source
Samaná Bay	C1, C2, C4–C7	44–365	32-164	41–162	4–44	This study
	C3 (marine carbonate)	6–50	16–37	33–38	3–8	This study
Paranagua Estuarine System, Brasil		15-58	7–22	27–80	17–30	[36]
Hong Kong, China		20–79	12–33	53–292	22–98	[37]
St. Lawrence Harbour, Canada		37–99	22–64	201–563	33–134	[38]
Beibu Bay, South China		6–84	NR	5–112	7–49	[39]
Persian Gulf, Iran		58–141	70–196	46–107	18–95	[40]
Upper Continental Crust		92	47	67	17	[35]

In general, all samples collected near to river mouths (C1, C2, C4, C5, C6, and C7) showed higher values of trace elements like Cr, Ni, and Zn, probably due to enrichment by human activities in earth basins. However, the cores showed a specific grade of enrichment as a result of different human activities in each earth local basin.

3.2. Local processes and trace elements in sediment cores

In the last decade, the Bay of Samaná was significantly impacted by extreme weather events [18]. These extreme events increased the contributions of sediment by the rivers [19], with a noticeable rising of sediment accumulation in the bay (Figure 3).

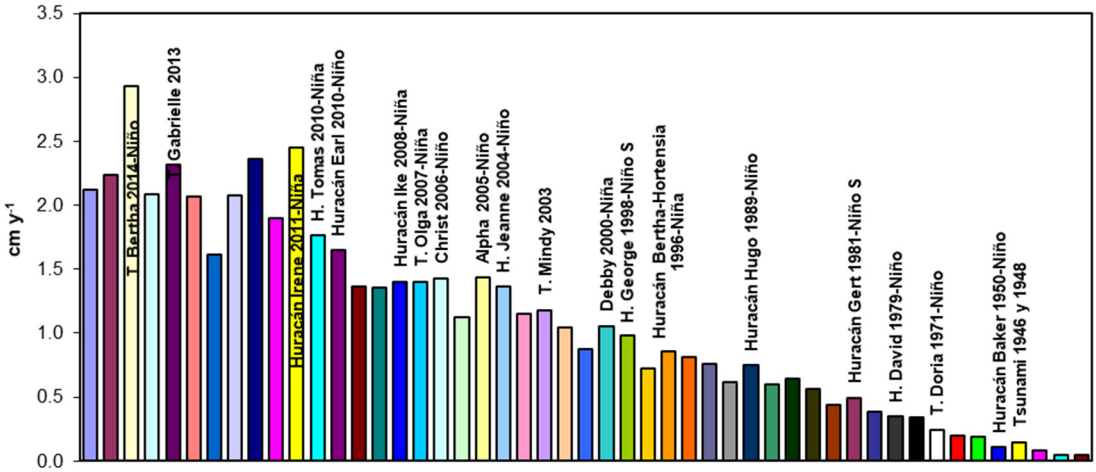

Figure 3. Relation of the Sedimentary Accumulation Rate (SAR) with extreme meteorological events during the period 1890–2016 that affected the bay of Samanà, Dominican Republic. See: https://ggweather.com/enso/oni.htm.

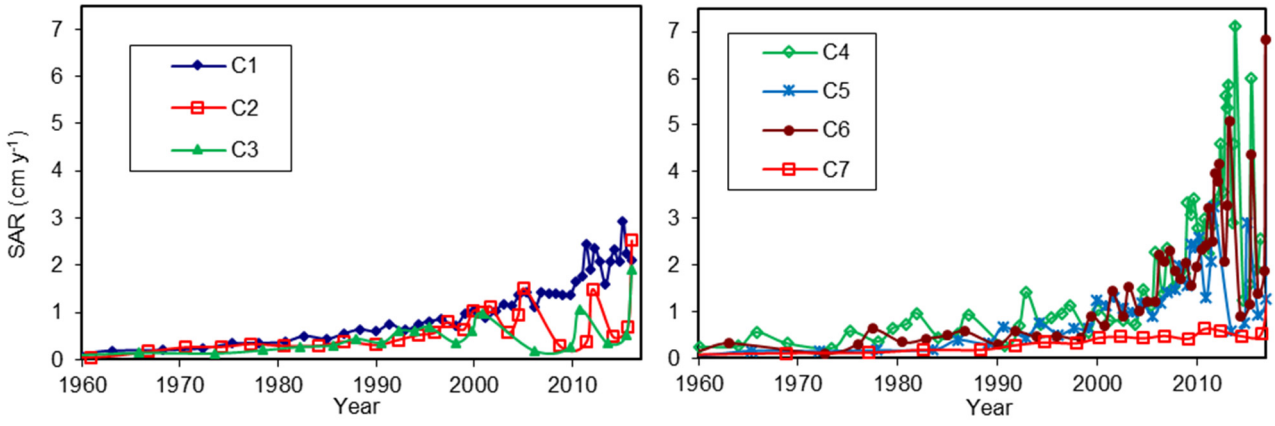

Figure 4. Graphs of the SAR of the cores collected in the Bay of Samaná (Delanoy et al., 2019). The dating was from 1890; while the data in the charts are only from 1960, for better visualization.

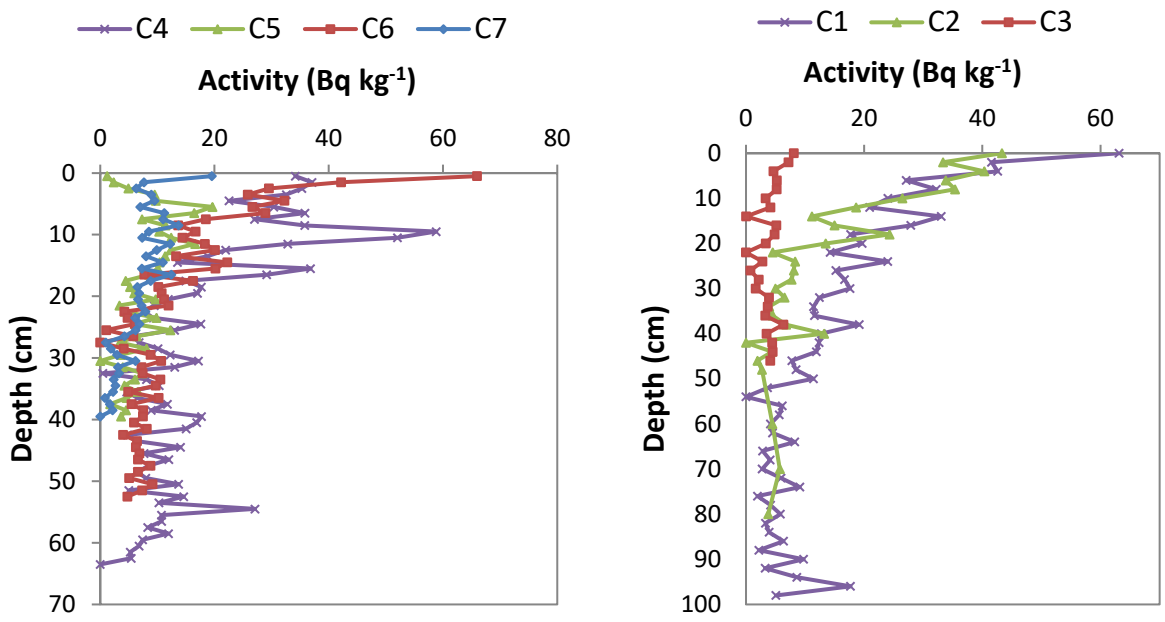

Figure 5. Variation of ^{210}Pb activity with depth in cores 1, 2 and 3, left. Cores 4, 5, 6 and 7, right.

The estimated sedimentary accumulation rate (SAR) in each core is shown in Figure 4 [1]. The values were estimated from the excess of ^{210}Pb in each sediment core (Figure 5). The average SAR for the 2003 to 2016 was 1.8 cm per year (cm y^{-1}) at the site of the C1 core (Figure 4); the Great Estero and the land of Lower Yuna have historically caused depositions in the river [41]. In the period 2003 to 2019, the Yuna River has made an intrusion of sediment displacing 2.38 km^2 of the bay (Figure 6) [42], Fe increased with depth in the C2 core and Ca increased slightly, while Al and Si decreased [1]. Apparently, due to a change in the water source of the sediment [16], supply being derived from two outlets, Yuna and Yuna-Barracote. In the C2 core, Ni and Cr exceeded the limits for sediment to be considered non-toxic (Table 3).

With an average SAR in the 2003 to 2016 period of 0.72 cm y^{-1}, core C3, taken North of Miches alongside an Hg-loaded galleon sunk in 1724 during a storm [43], Hg was not detected in the first 10 cm (Table 2), while in sections beyond 10 cm depth they registered the highest value over tolerable limits [1].

Between 1998 and 2011, the Samaná River, in the port of the same name (core C4), contributed the highest SAR due to a barrier that prevented sediment from spreading into the bay (Figure 4). In the port of Samaná (Samaná River), the C4 core was extracted with an average SAR in the period 2003 to 2017 of 3.1 cm a^{-1} (Figure 4) where Ca decreased with depth. A change from 22–43 cm in the sedimentation regime was observed under terrific influence of the Samaná River collecting the wastewater from Santa Bárbara de Samaná [1]. The trace elements, such as Hg, Pb, Ni and Cr, in several sections exceeded toxicity values (Tables 2 and 3).

Figure 6. Mouth of the Yuna River. The blue line represents the coastline from 2003, the yellow line from 2011, and the violet line from 2017. The riverbed was always the same due to its channeling. Between 2003 and 2011, 2.00 km^2 of the bay were lost, from 2003–2017 the loss was 2.17 km^2. All losses were caused by the entry of sediments from the Yuna River. Source: Google Earth, left; Photo: Landsat 8. https://landlook.usgs.gov/landlook/viewer.html, right.

The Yabón River flows into this area, near the municipality of Sabana de la Mar, and its main basin is in the eastern mountain range formed by karst and volcanic rocks. The chemical elements of the C5 core from 0–64 cm have changes, but from 60 cm the values remain constant [1]. Cr and Ni are the trace elements that exceeded the permissible exposure limit and effect threshold level (Table 3). The average SAR in the C5 core during 2003 to 2016 was 1.8 cm y^{-1} (Figure 4); from 2003–2019 the sediments occupied 0.13 km^2 of the bay (Figure 6).

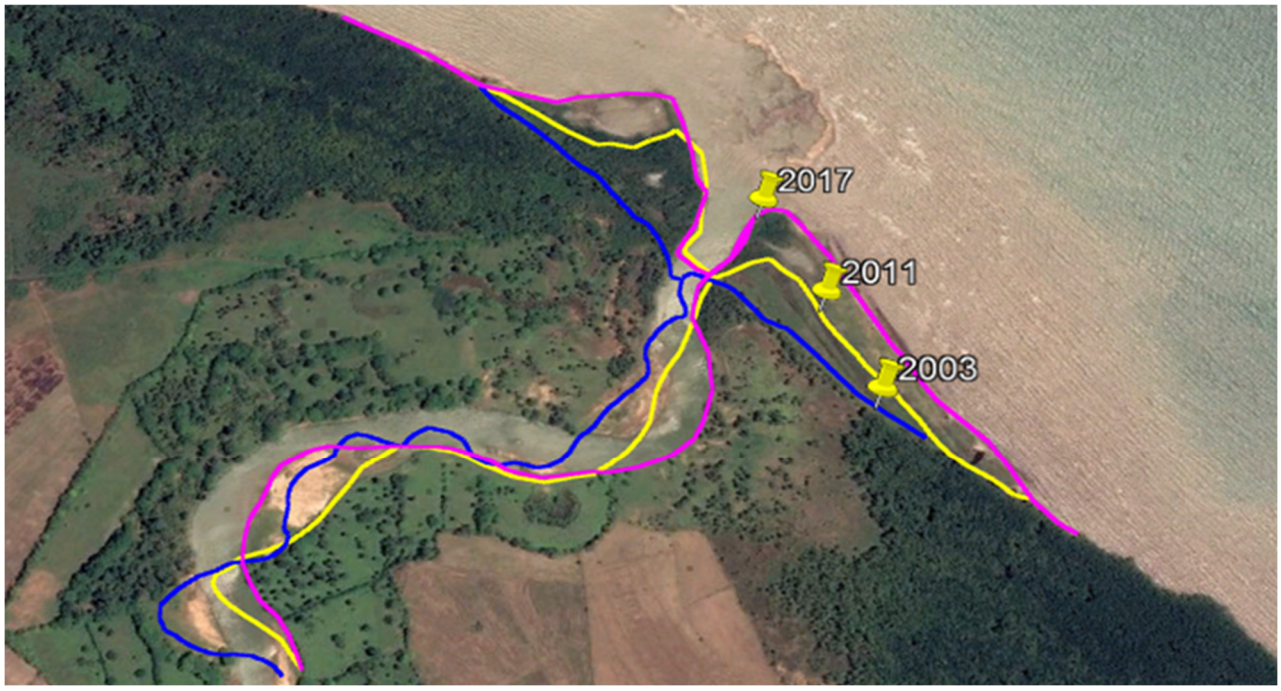

Figure 7. Mouth of the Yabón River. The blue line represents the right bank of the river and the coastline from 2003, the yellow line from 2011, and the violet from 2017. From 2003–2011, 0.10 km^2 of the bay were lost, from 2003–2017 the loss was 0.12 km^2. All losses were caused by sediments from the Yabón River. Source: Google Earth. Photo: Lansat 8.

In the C6 core that corresponds to the deposition of the sediment of the Caño Hondo River, in the bay of San Lorenzo, the average SAR reached 2.5 cm y^{-1} in the period 2003–2016. The sediments came from Los Haitises National Park, formed by karst rocks, dragged along the Caño Hondo River (core C6), deposited in the San Lorenzo Bay, which limits their spread. As in the C5 core, in the cases Ni and Cr exceeded the toxicity limits.

At the mouth of the La Yeguada River in Miches, the C7 core consisting of calcium carbonate with an average SAR during the 2003–2016 period of 0.6 cm y^{-1}. In this zone, from 2003–2019, the sediments occupied only 0.01 km^2 of the bay (Figure 8). In the first 10 cm deep was registered the highest value of trace elements over the tolerable limits (Table 3). Majority elements, as well as trace elements of Pb and Cr, vary according to the sedimentation rate. The C7 core has the same behavior as C5 and C6 cores due to the geological characteristics of its basins.

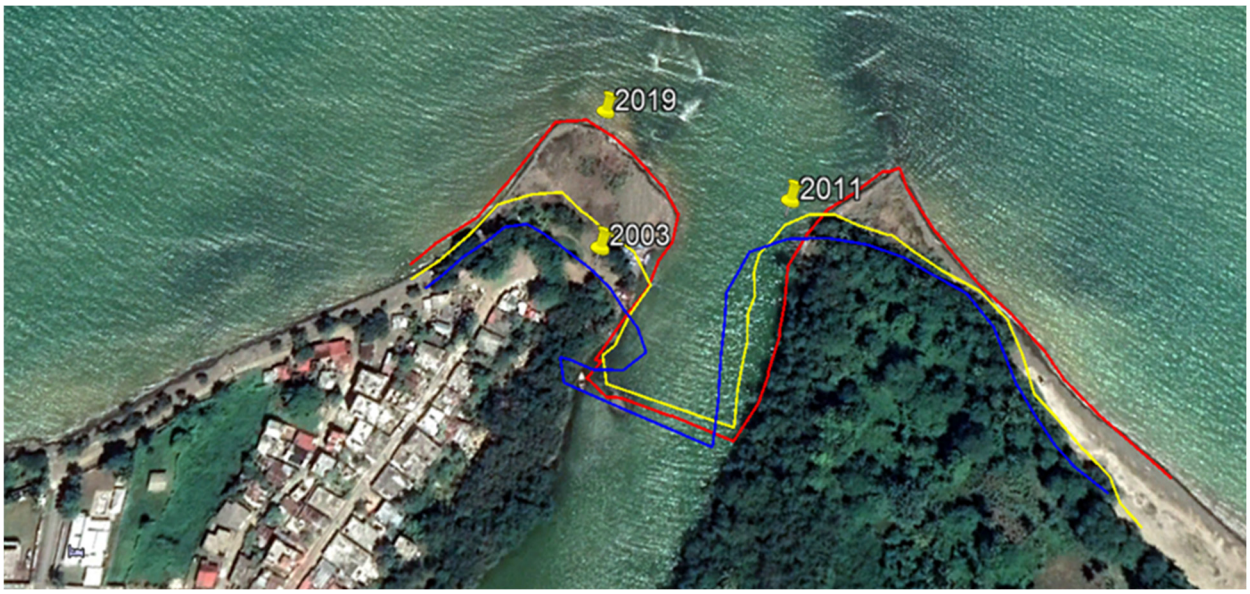

Figure 8. Mouth of the Yeguada River. The blue line represents the coastline from 2003, the yellow line from 2011, and the red line from 2019. Between 2003 and 2019, 0.01 km^2 of the bay were lost due to the entry of sediments contributed by the Yeguada River. At low tide, the river is closed to the sea by a sandbar. Source: Google Earth. Photo: Landsat 8.

In general, the Yuna River most abundantly contributes to the sedimentation of the bay, followed by the Yabón River, then the Samaná, Caño Hondo, and finally La Yeguada. From the North, other rivers and streams also make their contributions, with Los Cacaos having the highest incidence of sedimentation in the bay next to Samaná. The Yabón River is the next highest contributor, since the sediment has little mobility due to the granulometry [24], accumulating a short distance from the mouth (Figure 7). In contrast, sediment from the Yuna River has greater mobility spreading over a wider area (Figure 6). It was observed that the SAR has been increasing in all cores associated to how anthropogenic activities, such as agriculture, livestock, mining, and deforestation, impact the river basin and by the increase of the extreme weather events in the last decade in the northwest region of Dominican Republic.

4. Conclusions

From 2003 to 2016, Hispaniola Island was subjected to a period of great storms and hurricanes, which caused the Bay of Samaná to receive large amounts of sediment in its area, according to its watersheds. The SAR determined in the cores taken show large amounts of sediment deposited in the bay by rivers and streams, resulting in a decrease in the bay area, as well as its depth in the areas of sediment deposition.

It was inferred that much of this sediment contained toxic trace elements (Table 3) that exceeded the values of the SQuiRTs-NOAA table in significant quantities, and the health of the ecosystem will depend on the bioaccumulation capacity or tolerance of the species that inhabit the bay. The bay area has been gradually decreasing: between 2003 to 2019, the sediment from Yuna

and Yabon Rivers has occupied 2.38 km^2 and 0.13 km^2 of the bay, respectively, and the bottom of the bay in the vicinity has also been reduced. The reductions, all measured in the same period, were 44 cm for the C1 core, 12 cm for the C3 core, 32 cm for the C4 core, 38 cm for the C5 core, 27 cm for the C6 core, and 9 cm for the C7 core. The pronounced hydrometeorological activity in this period associated with climate change marked this accelerated sedimentation process of the Bay of Samaná, as well as other regions of the Dominican Republic, such as the Lake Enriquillo basin.

Acknowledgments

The authors would like to thank the reviewers for their thoughtful comments and efforts, which contributed to improving our manuscript. We also want to thank the staff of the Ministry of Higher Education, Science and Technology. Universidad Autónoma de Santo Domingo. Dr. Plácido Gómez, Dr. Carlos Rodríguez, MsC. Miledy Alberto, Radhamés Silverio, Master Idalia Acevedo, Lic. Domingo Mercedes, Lic. Isabel Ulloa, for financial support and management. Dr. Carlos M. Alonso Hernández, MsC Zoraida Zapata, MsC. Miguel Gomez Batista, Lic. Marcos Casila, Osvaldo Suárez, Juan Pablo González for their participation in the sampling; Msc. Nelphy de la Cruz, Yamileza Herrera, Queiroz Portorreal, Droniguiel Jiménez, for participation in the preparation and analysis of the samples. Andrés María Moreta Rosario for collaboration in preparing maps and graphs.

Conflict of interest

All authors declare no conflicts of interest in this paper.

References

1. Delanoy R, Díaz-Asencio M, Méndez-Tejeda R (2019) Effect of Extreme Weather Events on the Sedimentation of the Bay of Samaná, Dominican Republic (1900–2016). *J Geogr Geol* 11: 56–73.
2. Bionini W, Hargraves R, Shagan R (1984) The Caribean-South American Plate Boundary and Regional Tectonic. *Geol Soc Am Mem* 162.
3. Bird J (1980) Plate Tectonics. Select papers from Publications of American Geophysical Union, 2 Eds., Washington. D.C.
4. Eptisa (2004) Programa SYSMIN. Informe de la unidad hidrogeológica de la península de Samaná.
5. Dolan J, Mann P, De Zoeten R, et al. (1991) Sedimentologic, stratigraphicand tectonic synthesis of Eocene-Miocene sedimentary basins, Hispañiola and Puerto Rico, In: Mann P, Draper G, Lewis J, *Geologic and tectonic development of the North America-Caribbean Plate boundary in Hispañiola*. Geological Society of America Special Paper 262: 217–263.
6. Hippensteel SP, Eastin MD, Garcia WJ (2013) The geological legacy of Hurricane Irene: Implications for the fidelity of the paleo-storm record. *GSA Today* 23: 4–10.

7. Díaz de Neira JA, Braga JC, Mediato J, et al. (2015) Plio-Pleistocene palaeogeography of the Llanura Costera del Caribe in eastern Hispaniola (Dominican Republic): Interplay of geomorphic evolution and sedimentation. *Sediment Geol* 325: 90–105.
8. Trefethen JM (1981) *Geología para Ingenieros*. Décima edición, Cia. Editorial Continental, México.
9. Brenner M, Binford MW (1988) A sedimentary record of human disturbance from Lake Miragoane, Haiti. *J Paleolimnol* 1: 85–97.
10. Alonso-Hernández CM, Díaz-Asencio M, Gómez-Batista M, et al. (2016) Radiocronología de sedimentos marinos y su aplicación en la comprensión de los procesos de contaminación ambiental en ecosistemas marinos cubanos. *Nucleus* 60: 35–40.
11. Rozanski K, Stichler W, Gonfiantini R et al. (1992) The IAEA ^{14}C Intercomparison exercise 1990. *Radiocarbon* 34: 506–519.
12. Sánchez-Cabeza M, Ruiz-Fernández JA, Díaz-Asencio A (2012) Radiocronología de sedimentos costeros utilizando ^{210}Pb: modelos, validación y aplicaciones. Vienna: IAEA.
13. Salamanca M, Jara B (2003) Distribución y acumulación de plomo (Pb y ^{210}Pb) en sedimentos de los fiordos de la XI región, Chile. *Cienc Tecnol Mar* 26: 61–71.
14. Rodríguez Vegas E, Gascó Leonarte C, Schmid T, et al. (2014) Estudio Preliminar sobre el uso de los radionúclidos ^{137}Cs y ^{210}Pb y las Técnicas de Espectrorradiometría como Herramientas para determinar el Estado de Erosión de suelos. *Inf Téc Ciemat* 1297.
15. Cisternas M, Torres L, Urrutia R, et al. (2000) Comparación ambiental, mediante registros sedimentarios, entre las condiciones prehispánicas y actuales de un sistema lacustre. *Rev Chil Hist Nat* 73: 151–162
16. Armstrong-Altrin JS, Botello AV, Villanueva SF, et al. (2019) Geochemistry of surface sediments from the north-western Gulf of Mexico: implications for provenance and heavy metal contamination. *Geol Q* 63: 522–538.
17. Fourth National Climate Assessment (NCA4) (2018) Available from: https://www.globalchange.gov/nca4.
18. Null J (2017) El Niño and La Niña Years and Intensities. Based on Oceanic Niño Index (ONI), CCM. Available from: https://ggweather.com/enso/oni.htm.
19. Ramón DA, Méndez-Tejeda R (2017) Hydrodynamic Study of Lake Enriquillo in Dominican Republic. *J Geosci Environ Prot* 5: 115–124.
20. Ortega-Ariza D, Franseen EK, Santos-Mercado H, et al. (2015) Strontium Isotope Stratigraphy for Oligocene-Miocene Carbonate Systems in Puerto Rico and the Dominican Republic: Implications for Caribbean Processes Affecting Depositional History. *J Geol* 123: 539–560.
21. Mercier G, Duchesne J, Blackburn D (2001) Prediction of metal removal efficiency from contaminated soils by physical methods. *J Environ Eng* 127: 348–358.
22. Loring DH, Rantala RTT (1992) Manual for the geochemical analyses of marine sediments and suspended particulate matter. *Earth-Sci Rev* 32: 235–283.
23. Díaz de Neira JA, Braga JC, Mediato J, et al. (2017) Evolución paleogeográfica reciente del sector oriental de La Española. *Bol Geol Min* 128: 675–693.

24. Anaya-Gregorio A, Armstrong-Altrin JS, Machain-Castillo ML, et al. (2018) Textural and geochemical characteristics of late Pleistocene to Holocene fine-grained deep-sea sediment cores (GM6 and GM7), recovered from southwestern Gulf of Mexico. *J Palaeogeogr* 7: 253–271.
25. Pérez-Estaún A, Hernaiz Huerta PP, Lopera E, et al. (2007) Geología de la República Dominicana: de la construcción de arco-isla a la colisión arco-continente. *Bol Geol Min* 118: 157–174.
26. Senz JG, Monthel J, Díaz de Neira JA, et al. (2007) La estructura de la Cordillera Oriental de la República. *Bol Geol Min* 118: 293–311.
27. Hernaiz Huerta PP (2004) Mapa Geológico de la Hoja a E. 1:50.000. 5871-I (La Descubierta) y Memoria correspondiente. Proyecto de Cartografía Geotemática de la República Dominicana. Programa SYSMIN. Dirección General de Minería, Santo Domingo.
28. Meyers PA, Teranes JL (2001) Sediment organic matter. In: Last WM, Smol JP (eds.). *Tracking environmental change using lake sediments*. Kluwer Academic Publishers, Holanda, 239–269.
29. Rudolph A, Ahumada R, Hernández S (1984) Distribución de la materia orgánica, carbono orgánico, nitrógeno orgánico y fósforo total en los sedimentos recientes de la Bahía Concepción, Chile. *Biol Pesq* 13: 71–82.
30. Rodríguez L, Jiménez A, Grau A (1996) Separación del ^{210}Pb, ^{210}Bi y ^{210}Po mediante columna de cambio iónico y su calibración por centelleo líquido. *Ciemat* 27: 1–30.
31. Lozano RL, San Miguel EG, Bolívar JP (2011) Assessment of the influence of in situ ^{210}Bi in the calculation of in situ ^{210}Po in air aerosols: Implications on residence time calculations using ^{210}Po/^{210}Pb activity ratios. *J Geophys Res* 116: D08206.
32. Mosqueda Peña F (2010) *Desarrollo de procedimientos para la determinación de radioisótopos en muestras ambientales mediante técnicas de bajo recuento por centelleo líquido y radiación Cerenkov*. Universidad de Huelva. Tesis Doctoral.
33. IAEA (1989) Isotopes of Noble gases as tracers in environmental studies. Proceeding Consultants Meeeting, Agency International, Vienna.
34. Buchman MF (1999) NOAA Screening Quick Reference Tables. In: National Oceanic and Atmospheric Administration, NOAA HAZMAT Report, Seattle WA, Coastal protection and restoration division, 12.
35. Rudnick RL, Gao S (2003) Composition of the Continental Crust. In: Rudnick RL, *Treatise on Geochemistry* 3: 1–64.
36. Choueri RB, Cesar A, Torres RJ, et al. (2009) Integrated sediment quality assessment in Paranaguá Estuarine System, Southern Brazil. *Ecotoxicol Environ Saf* 72: 1824–1831.
37. Zhang X, Man X, Jiang H (2015) Spatial distribution and source analysis of heavy metals in the marine sediments of Hong Kong. *Environ Monit Assess* 187: 1–12.
38. Pourabadehei M, Mulligan CN (2016) Effect of the resuspension technique on distribution of the heavy metals in sediment and suspended particulate matter. *Chemosphere* 153: 58–67.
39. Dou Y, Li J, Zhao J, et al. (2013) Distribution, enrichment and source of heavy metals in surface sediments of the eastern Beibu Bay, South China Sea. *Mar Pollut Bull* 67: 137–145.
40. Pejman A, Bidhendi GN, Ardestani M, et al. (2015) A new index for assessing heavy metals contamination in sediments: A case study. *Ecol Indic* 58: 365–373.

41. Dolan JF, Mann P (1998) *Active Strike-slip and Collisional Tectonics of the Norther Caribbean Plate Boundary Zone*. Department of Earth Sciences University Southern of California. The Geological Society of America. Special Paper 326.
42. Mann P, Burke K, Matumoto T (1984) Neotectonics of Hispañiola: plate motion, sedimentation, and seismicity at a restraining bend. *Earth Planet Sci Lett* 70: 311–324.
43. Fernández-Domingo JI (2010) *Los Tesoros del Mar y su Régimen Jurídico*. Biblioteca Iberoamericana de Derecho, Madrid, Buenos Aires.

AIMS Press